Low-energy local density of states of the 1D Hubbard model

Stefan A. Söffing,[1,2] Imke Schneider,[3] and Sebastian Eggert[1,2]

[1] *Dept. of Physics and Research Center OPTIMAS, Univ. Kaiserslautern, D-67663 Kaiserslautern, Germany*
[2] *MAINZ Graduate School of Excellence*
[3] *Institut für Theoretische Physik, Univ. Dresden, D-01062 Dresden, Germany*

We examine the local density of states (DOS) at low energies numerically and analytically for the Hubbard model in one dimension. The eigenstates represent separate spin and charge excitations with a remarkably rich structure of the local DOS in space and energy. The results predict signatures of strongly correlated excitations in the tunneling probability along finite quantum wires, such as carbon nanotubes, atomic chains or semiconductor wires in scanning tunneling spectroscopy (STS) experiments. However, the detailed signatures can only be partly explained by standard Luttinger liquid theory. In particular, we find that the effective boundary exponent can be negative in finite wires, which leads to an increase of the local DOS near the edges in contrast to the established behavior in the thermodynamic limit.

Interacting one-dimensional quantum wires are well studied examples of systems in which the Fermi liquid paradigm of electron-like quasi-particles is known to break down. Luttinger liquid theory predicts that strong correlations lead to the remarkable phenomenon of separate spin- and charge-density waves as the fundamental collective excitations in one dimension at low energies [1]. Experimental confirmation for this picture has long been controversial, but now there is some evidence for separately dispersing spin and charge resonances for quantum wires on semiconductor hetero-structures [2, 3], quasi one-dimensional crystals [4] and self-organized atomic chains [5] as a function of momentum. The density of states (DOS) has also been analyzed by scanning tunneling spectroscopy (STS) in carbon nanotubes [6–8] and self-organized atomic chains [9]. This immediately invites the question, if there are characteristic signatures from standing waves of separate spin and charge densities, that can potentially be detected in *locally* resolved STS experiments in finite wires. Detailed Luttinger liquid calculations near boundaries exist, which predict corresponding wave-like modulations in the local DOS and a sharp reduction of the DOS near boundaries [10–14]. However, it is far from clear if these signatures are robust in realistic lattice systems, since even minimalistic models like the Hubbard chain are not perfect Luttinger liquids. The two main reasons for possible discrepancies are that first of all the assumed degeneracy of spin and charge modes in the low energy spectrum can never be exact and will be lifted by band curvature and other effects. Secondly, it is known that strong logarithmic corrections will arise from a spin umklapp operator which is generically present in 1D electron systems with SU(2) invariant interactions [15–17].

The most relevant minimalistic lattice model is the Hubbard chain

$$H = -t \sum_{\sigma,\, x=1}^{L-1} \left(\psi^\dagger_{\sigma,x} \psi_{\sigma,x+1} + \text{h.c.} \right) + U \sum_{x=1}^{L} n_{\uparrow,x} n_{\downarrow,x}, \quad (1)$$

which captures the main aspects of interacting one dimensional electron systems. This model shows signatures of spin-charge separation in numerical simulations of the momentum resolved DOS [18], which is the central quantity relevant for photoemission experiments. In this paper we will now analyze the *local* DOS as a function of position and energy which in turn is relevant for STS experiments.

Recently, several numerical density matrix renormalization group (DMRG) studies considered the local DOS for *spinless* lattice fermion models in one dimension [19–21], where there is no spin and charge separation. Therefore, the complications mentioned above do not arise and the agreement with theory is close to perfect in that case. As we will show here, the local DOS for a *spinful* electron system away from half-filling is much more complex and some key features of the Luttinger liquid theory are strongly renormalized.

The observable of interest is the local DOS to tunnel an electron with spin up at a certain energy ω into the wire,

$$\rho(x,\omega) = \sum_\alpha \left| \langle \omega_\alpha | \, \psi^\dagger_{\uparrow,x} \, |0\rangle \right|^2 \delta(\omega - \omega_\alpha) \quad (2)$$

$$= \frac{1}{\pi} \operatorname{Im} \int_0^\infty e^{\,\mathrm{i}\omega t} \, \mathrm{i} \langle \psi_{\uparrow,x}(t) \psi^\dagger_{\uparrow,x}(0) \rangle \, \mathrm{d}t. \quad (3)$$

Here, the fermion operator $\psi^\dagger_{\uparrow,x}$ creates a particle at position x on top of the groundstate $|0\rangle$ and the sum runs over all states $|\omega_\alpha\rangle$ with one additional electron.

In the following we will compare analytical calculations for the local DOS from Luttinger liquid theory with simulations using the numerical DMRG algorithm [22, 23]. For the matrix elements in Eq. (2) we use a multi-target DMRG with a large number of target states in two different particle number sectors [19] and keep track of all local fermion creation operators.

In order to identify the separate spin and charge excitations, we first focus on the energy spectrum $\Delta\omega = \omega_\alpha - \omega_0$

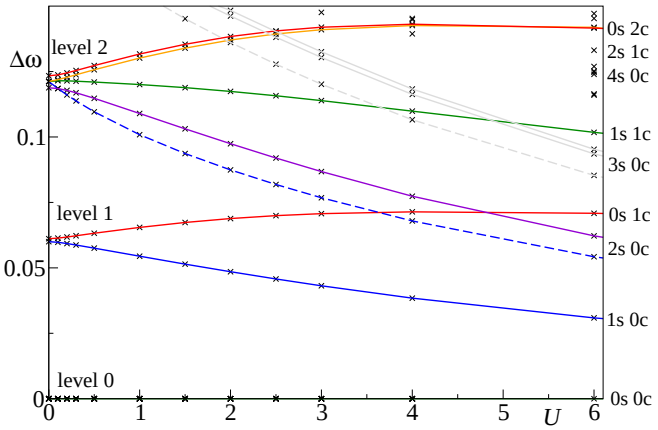

FIG. 1: (Color online) Energies $\Delta\omega = \omega_\alpha - \omega_0$ as a function of U for excited states with $N_\uparrow = N_\downarrow + 1 = 31$ particles on a lattice of length $L = 90$. The quantum numbers on the right indicate the corresponding mode $\{m_s, m_c\}$. Dashed lines correspond to $S = 3/2$ states. For larger U, excitations from level 3 (3s,0c) and level 4 also appear in the low energy spectrum.

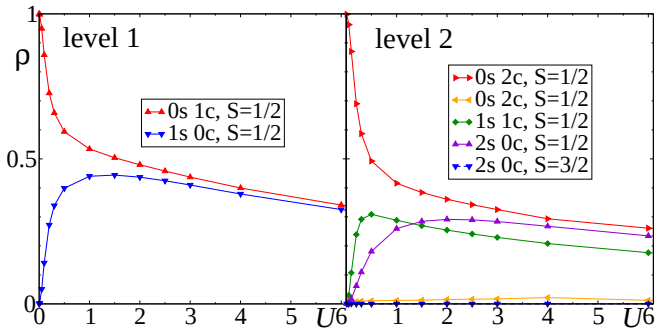

FIG. 2: (Color online) Total DOS for the excitations of the first two levels from Fig. 1.

for finite wires of length L as a function of interaction U as shown in Fig. 1 in units of $t = 1$. The ground state $|0\rangle$ is assumed to be a filled Fermi sea with total magnetization $S^z = 0$, so that all particle excited states $|\omega_\alpha\rangle$ have $N_\uparrow = N_\downarrow + 1$ particles and total spin z-component $S^z = 1/2$.

For $U = 0$ all excitations are described by simple products of fermion operators $c^\dagger_{\sigma,n} = \sqrt{\frac{2}{L+1}} \sum_x \psi^\dagger_{\sigma,x} \sin(k_F + k_{n+1})x$ where $k_n = n\frac{\pi}{L+1}$ and $|\omega_0\rangle = c^\dagger_{\uparrow,0}|0\rangle$ is the lowest energy particle excitation. Since the spectrum is approximately linear $\Delta\omega \sim v_F(k - k_F)$, a state involving several fermion operators (i.e. a multi-particle excitation) is nearly degenerate with a single particle excitation at $U = 0$ if the sum of excited wavenumbers is the same, which results in quantized fermion levels shown in Fig. 1. For example in level 1, the two states $c^\dagger_{\uparrow,1}|0\rangle$ and $c^\dagger_{\uparrow,0}c^\dagger_{\downarrow,0}c_{\downarrow,-1}|0\rangle$ both have approximately the same energy $\omega_1 - \omega_0 \approx v_F k_1$. In general there are many multi-particle states in each level n, but only one single particle state $c^\dagger_{\uparrow,n}|0\rangle$ carries all the DOS if $U = 0$.

The situation changes for finite U. Now all states may potentially carry spectral weight in the DOS and the near-degeneracy of the levels is lifted. According to the Luttinger liquid picture the states are now described by integer spin and charge quantum numbers $\{m_s, m_c\}$ with energies $\omega_{m_s,m_c} = (m_s v_s + m_c v_c)\frac{\pi}{L+1}$ in terms of the spin and charge velocities $v_s \le v_c$ [1, 14]. The spectrum in Fig. 1 shows a regular spin and charge spacing with quantum numbers shown on the right. For each spin/charge mode $\{m_s, m_c\}$ there can be several states with approximately the same energy. The number of states in each mode is given by the number of ways it can be created by boson creation operators $b^\dagger_{m,\nu}$, i.e. the product of the integer partitions of m_s and m_c. For example, for the mode $0s\ 2c$ in Fig. 1, we have $m_c = 2 = 1 + 1$ corresponding to the two states created by $b^\dagger_{2,c}$ and $(b^\dagger_{1,c})^2$, respectively, which indeed have almost the same energy. On the other hand, the near degeneracies of spin modes (e.g. $2s\ 0c$) are significantly split in Fig. 1 by well-known logarithmic corrections as will be discussed below [15–17].

Regarding the DOS it is now interesting to explore how the total spectral weight is distributed among the excited states. The compact answer from Luttinger liquid theory is that the summed up DOS in each mode $\{m_s, m_c\}$ should be proportional to a powerlaw of the corresponding energy, but there are no predictions how the DOS is distributed among the states within each mode. For the lowest energy modes the situation is still simple, since the first level corresponds to one spin and one charge state, which should have roughly the same DOS of 1/2 each for small U according to theory. However, the numerical results in Fig. 2 already demonstrate obvious deviations from this prediction, since the charge mode has a much larger DOS for small U. The reason for this discrepancy comes from the non-linear band curvature, which lifts the degeneracy for finite L even at $U = 0$, so that the interaction has to overcome this energy splitting. Indeed for cases where the two states are exactly degenerate at $U = 0$ (e.g. in the thermodynamic limit) the spin and charge states have comparable DOS even for infinitesimally small U. As can be seen in Fig. 2 for $L = 90$ the charge state dominates for $U \lesssim 0.5$, which would imply that for $U \lesssim 10\frac{v_s \pi}{L}$ the band curvature is dominant over the interaction effects. The next five states from the second fermion level in Fig. 2 show a similar crossover behavior with U. Nonetheless, features in the *local* DOS will clearly show the interaction effects even in the crossover region as we will see below.

In the $0s\ 2c$ and the $2s\ 0c$ modes there are two states each as expected. However, only one of the states in each mode contributes the overwhelming majority of the DOS, while the other state would be practically invisible in an STS experiment. The reason that some states in a

given mode have zero DOS can sometimes be linked to exact symmetries, such as the SU(2) symmetry of generic Coulomb interactions. In particular, all particle excitations $|\omega_\alpha\rangle$ in the $S^z = 1/2$ sector are representatives of SU(2) multiplets. The lowest energy state $|\omega_0\rangle$ always belongs to a doublet with $S = 1/2$. Excitations with charge bosons $b^\dagger_{\ell,c}$ never change the total spin, but excitations with spin bosons $b^\dagger_{\ell,s}$ may generate higher spin values, which can be calculated using the commutation rules of the non-abelian SU(2)-Kac-Moody algebra [15], since the spin bosons correspond to the modes of the SU(2) current along the z-direction as discussed in the appendix. For example the lowest energy $S = 3/2$ state is given by the spin boson excitation $\frac{1}{\sqrt{3}}[(b^\dagger_{1,s})^2 - b^\dagger_{2,s}]|\omega_0\rangle$ with $m_s = 2$ which is plotted as a dashed line in Fig. 1. Such a total spin analysis can be performed for a large number of excitations (see also appendix), which is useful since states with $S > 1/2$ must have zero DOS due to angular momentum addition rules. For example in the fifth spin mode $5s\ 0c$, there are 7 states, three of which have total spin $S = 3/2$ and exactly zero DOS. Interestingly, three more states carry only very small spectral weight, so that only one state dominates for this mode. This indicates that the eigenstates remain the same in terms of their bosonic expressions even for $U \neq 0$. For charge modes there is also exactly one state which carries the overwhelming weight in each mode, but the DOS of the other states is finite and generally increases with U.

For a complete analysis it is now useful to turn to the *local* DOS $\rho_{m_s,m_c}(x)$ for each mode $\{m_s, m_c\}$. Bosonization predicts that the local DOS for a given mode is composed of a uniform and an oscillating product of spin and charge contributions [14]

$$\rho_{m_s,m_c}(x) = |c_x|^2 \left[\rho^{\rm u}_{s,m_s}(x)\rho^{\rm u}_{c,m_c}(x) - \cos(2k_{\rm F}x)\rho^{\rm o}_{s,m_s}(x)\rho^{\rm o}_{c,m_c}(x)\right]. \quad (4)$$

In what follows we will focus only on the uniform part of the local DOS in Eq. (4), since the quickly oscillating $2k_F$-terms cannot be easily resolved in an STS experiment yet. The amplitudes $\rho^{\rm u}_{\nu,m}(x)$ are slowly varying and can be predicted by a simple recursive formula for spin and charge ($\nu = c, s$) separately [14],

$$\rho^{\rm u}_{\nu,m}(x) = \frac{1}{m}\sum_{\ell=1}^{m} \rho^{\rm u}_{\nu,m-\ell}(x)\gamma^{\rm u}_{\nu,\ell}(x), \quad (5)$$

$$\text{where} \quad \gamma^{\rm u}_{\nu,\ell}(x) = a_\nu + b_\nu \cos(2k_\ell x). \quad (6)$$

Here we have defined spin and charge exponents $a_\nu = (1/K_\nu + K_\nu)/4$ and $b_\nu = (1/K_\nu - K_\nu)/4$ in terms of the respective Luttinger parameters K_ν for $\nu = c, s$. The overall prefactor $|c_x|^2 \propto (\sin\frac{\pi x}{L+1})^{b_c+b_s}$ in Eq. (4) does not depend on energy and serves as normalization so that $\rho^{\rm u/o}_{\nu,m=0} = 1$. It is straight-forward to see that the recursive formula results in powerlaws for the DOS in the bulk $\rho \propto \omega^{a_c+a_s-1}$ for $L \to \infty$ [14, 24]. In addition, the formula predicts slow wavelike modulations in the local DOS due to the second term in Eq. (6), which also survive in the thermodynamic limit near the edge [10].

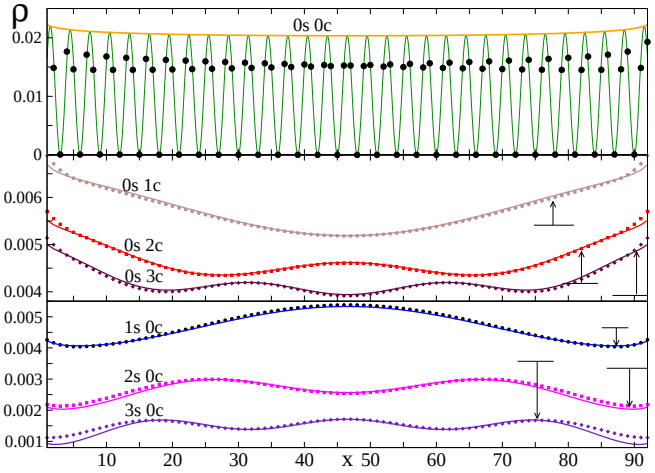

FIG. 3: (Color online) The local DOS of the first few modes for $L = 92$ and $U = 1$. Points are DMRG data and lines are theoretical predictions for $K_c = 0.9081$ and $K_s = 1.16$ adjusted by a shift as indicated by arrows (see text). Top: Local DOS for $|\omega_0\rangle$. The thick line corresponds to $2|c_x|^2$. Lower plots: Uniform part of the local DOS for the first few charge and spin modes.

The local DOS from the DMRG data is shown in Fig. 3 for the first few modes at 1/3-filling. For the lowest excitation $|\omega_0\rangle$ the oscillating and uniform parts are the same and given by the prefactor $|c(x)|^2$. Already at first sight it is surprising to see that the local DOS for all modes increases slightly near the boundary, while previous works have predicted it to decrease according to the boundary exponent[10, 24, 25]. Indeed it must be emphasized that the local DOS does *not* fit the theoretical prediction. All curves should in principle be fit free, up to one overall normalization, since the local DOS of all levels follows from Eqs. (4)-(6), where the Luttinger parameters $K_c(U)$ and $K_s = 1$ are known from the thermodynamic Bethe ansatz. However, in Fig. 3 two important adjustments have been made: First the theoretical curves were shifted down for the charge modes and up for the spin modes in order to fit the numerical data (indicated by arrows). This adjustment was already observed in the crossover of the total DOS in Fig. 2 due to the competition of energy scales (band curvature vs. interaction) as argued above. Secondly, we find that the spin Luttinger liquid parameter must be chosen considerably larger than unity $K_s \approx 1.16$ for all spin modes in order to fit the numerical data corresponding to *attractive* behavior in the spin modes. This is especially surprising since the charge Luttinger parameter from Bethe ansatz $K_{\rm c} = 0.9081$ agrees perfectly with the data without any finite size adjustments. There are no other adjustable

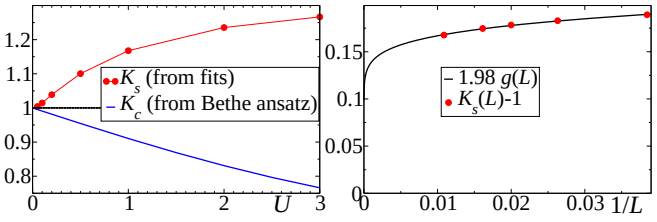

FIG. 4: (Color online) Left: Luttinger parameters K_c (line) from Bethe ansatz and K_s (points) from the fits to $\rho^{u}_{s,m=1}(x)$ as a function of U for $L = 92$. Right: Renormalization of K_s (points) at $U = 1$ with the system size L compared to Eq. (7).

parameters in the fits of Fig. 3, except for one overall normalization constant. In return, the results show that knowing the local DOS from (numerical) experiments, it is possible to extract the effective parameters K_s and K_c from the modulations of only the first spin and charge excited states according to Eqs. (4)-(6). The oscillating parts ρ^{o}_{ν} can be analyzed analogously and give the same results (not shown).

In Fig. 4 the behavior of the Luttinger parameters from the corresponding fits to the local DOS is shown as function of interaction and length at 1/3-filling. The charge parameter from Bethe ansatz K_c always agrees very well with the data without any additional adjustments. However, the observed spin parameter K_s is considerably larger than $K_s = 1$. Non-abelian bosonization predicts $K_s = 1$ for any SU(2) invariant model, but at the same time it is known that a marginal irrelevant operator causes corrections to the anomalous dimension which only vanish logarithmically slowly with $1/\ln L$ in the thermodynamic limit [15, 16]. In abelian bosonization such a correction can indeed effectively be modeled by a renormalizing spin Luttinger parameter [15–17, 26, 27]

$$K_s - 1 \propto g, \text{ with } g^{-1} + \frac{1}{2}\ln(g) = \ln(L/L_0) \qquad (7)$$

where L_0 is non-universal and depends on the model and the quantity of interest. As shown in Fig. 4 such a renormalization description is indeed consistent with our data for K_s. The parameter K_s increases with U at a given length L, but decreases slowly as the length is increased. The parameter K_s appears to be the same for all spin modes at a given U and L, i.e. independent of energy ω. The renormalization of K_s is very slow, so that exponentially large systems are required to observe the thermodynamic limit $K_s \to 1$. The fit parameters for $K_s \approx 1 + 1.98g$ with $\ln L_0 \approx -6$ are outside the range what would normally be expected for a spin chain model [17]. Therefore, the particular form of the observed corrections remains a puzzle.

Nonetheless, the results of the logarithmic corrections have interesting consequences. In particular, the corrections are so large, that the boundary exponent $\alpha_B = (1/K_s + 1/K_c)/2 - 1$ may become negative if $K_s + K_c < 2K_sK_c$, i.e. $K_s - 1 \gtrsim 1 - K_c$ to lowest order in the correction, which is indeed the case for small $U \lesssim 2t$ at $L = 92$. This results in an *increase* of the local DOS for small energies ω and small distances x near the boundary, which is described by a weak powerlaw divergence $\rho \propto x^{b_s+b_c}\omega^{\alpha_B}$. Such a negative boundary exponent would also explain the recently observed anomalies in the boundary behavior for small interactions in functional renormalization group studies [28].

In conclusion, we have analyzed the local DOS of the Hubbard model in the low energy regime. Individual states can be classified by separate spin- and charge quantum numbers. We observe that typically only one eigenstate contributes the overwhelming majority of the local DOS in each spin/charge mode. The spin and charge Luttinger parameters K_s and K_c can be extracted from the modulations in the local DOS of individual excited states. While the charge parameter K_c agrees well with the Bethe ansatz, the spin Luttinger liquid parameter is attractive $K_s > 1$ due to large finite size corrections, which can only be neglected for exponentially long chain lengths. In fact, the corrections to K_s are unexpectedly strong and may even lead to negative boundary exponents for moderate interactions $U \lesssim 2t$. The common assumption that it is possible to generically use $K_s = 1$ due to SU(2) invariance is certainly not justified for the local DOS. In particular, for finite wires on conducting substrates the interactions may be reduced by screening, so that the charge Luttinger liquid parameter K_c may be close to one, while the spin Luttinger liquid parameters K_s can already be significantly increased, which leads to a negative boundary exponent. This would have quite dramatic consequences, since the DOS near the boundary determines the tunneling between connected wires and the renormalization of the conductivity through impurities [25], which will show an increase at low temperatures in this scenario.

We are thankful for useful discussions with A. Struck and M. Bortz. This work was supported by the DFG and the State of Rheinland-Pfalz via the SFB/Transregio 49 and the MAINZ graduate school of excellence.

[1] For a review, see J Voit, Rep. Prog. Phys. **58**, 977 (1995).
[2] O.M. Auslaender, H. Steinberg, A. Yacoby, Y. Tserkovnyak, B.I. Halperin, K.W. Baldwin, L.N. Pfeiffer, and K.W. West. Science, **308**, 88 (2005).
[3] Y. Jompol, C.J.B. Ford, J.P. Griffiths, I. Farrer, G.A.C. Jones, D. Anderson, D.A. Ritchie, T.W. Silk, and A.J. Schofield, Science **325**, 597 (2009).
[4] B. J. Kim, H. Koh, E. Rotenberg, S.-J. Oh, H. Eisaki, N. Motoyama, S. Uchida, T. Tohyama, S. Maekawa, Z.-X. Shen, and C. Kim, Nature Phys. **2**, 397 (2006).
[5] P. Segovia, D. Purdie, M. Hengsberger, and Y. Baer, Nature **402**, 504 (1999).
[6] J. Lee, S. Eggert, H. Kim, S.-J. Kahng, H. Shinohara,

and Y. Kuk, Phys. Rev. Lett. **93**, 166403 (2004).
[7] L.C. Venema, J.W.G. Wilder, J.W. Janssen, S.J. Tans, H.L.J. Temminck Tuinstra, L.P. Kouwenhoven, and C. Dekker, Science **283**, 52 (1999).
[8] S.G. Lemay, J.W. Janssen, M. van den Hout, M. Mooij, M.J. Bronikowski, P.A. Willis, R.E. Smalley, L.P. Kouwenhoven, and C, Dekker, Nature **412**, 617 (2001).
[9] C. Blumenstein, J. Schäfer, S. Mietke, S. Meyer, A. Dollinger, M. Lochner, X.Y. Cui, L. Patthey, R. Matzdorf, and R. Claessen, Nature Phys. **7**, 776 (2011).
[10] S. Eggert, H. Johannesson, and A. Mattsson, Phys. Rev. Lett. **76**, 1505 (1996).
[11] S. Eggert, Phys. Rev. Lett. **84**, 4413 (2000).
[12] F. Anfuso and S. Eggert. Phys. Rev. B, **68**, 241301(R) (2003).
[13] P. Kakashvili, H. Johannesson, and S. Eggert Phys. Rev. B **74**, 085114 (2006).
[14] I. Schneider and S. Eggert, Phys. Rev. Lett. **104**, 036402 (2010).
[15] I. Affleck, D. Gepner, H. J. Schulz, and T. Ziman, J. Phys. A **22**, 511 (1989).
[16] T. Giamarchi and H. J. Schulz, Phys. Rev. B **39**, 4620 (1989).
[17] S Lukyanov, Nucl. Phys. B **522**, 533 (1998).
[18] H. Benthien, F. Gebhard, and E. Jeckelmann, Phys. Rev. Lett., **92**, 256401 (2004).
[19] I. Schneider, A. Struck, M. Bortz, and S. Eggert, Phys. Rev. Lett. **101**, 206401 (2008).
[20] P. E. Dargel, A. Honecker, R. Peters, R. M. Noack, and T. Pruschke, Phys. Rev. B **83**, 161104 (2011).
[21] E. Jeckelmann, preprint arXiv:1111.6545 (2012)
[22] S.R. White, Phys. Rev. Lett. **69**, 2863 (1992).
[23] S.R. White, Phys. Rev. B **48**, 10345 (1993).
[24] A.E. Mattsson, S. Eggert, and H. Johannesson, Phys. Rev. B **56**, 15615 (1997).
[25] C.L. Kane and M.P.A. Fisher, Phys. Rev. B **46**, 15233 (1992).
[26] J. Sirker, N. Laflorencie, S. Fujimoto, S. Eggert, and I. Affleck, Phys. Rev. Lett. **98**, 137205 (2007).
[27] J. Sirker, S. Fujimoto, N. Laflorencie, S. Eggert, and I. Affleck, J. Stat. Mech. P02015 (2008).
[28] D. Schuricht, S. Andergassen, and V. Meden, preprint arXiv:1111.7174 (2012).

Appendix: Non-abelian Bosonization

In order to determine the total spin of an excitation it is useful to use non-abelian bosonization in the spin channel [15]. In this case the excitations are created by the modes of SU(2) currents J^a_m with $a = x, y, z$ obeying the Kac-Moody algebra

$$[J^a_m, J^b_n] = \mathrm{i}\varepsilon^{abc} J^c_{m+n} + \tfrac{1}{2} m \delta^{a,b} \delta_{m,-n} \tag{A.8}$$

The ground state is characterized by $J^a_m|\omega_0\rangle = 0,\ \forall\, m < 0$. The total spin operator is given in terms of the $m = 0$ currents

$$S^2 = \vec{J}_0 \cdot \vec{J}_0 = 2J^+_0 J^-_0 + J^z_0 + (J^z_0)^2 \tag{A.9}$$

where $J^\pm = J^x \pm \mathrm{i}J^y$. The current modes in the z-direction are related to the abelian spin bosons above by $J^z_m = \sqrt{\frac{m}{2}} b^\dagger_{m,s}$ and $J^z_{-m} = \sqrt{\frac{m}{2}} b_{m,s}$ for $m > 0$. It is therefore straight-forward to consider the total spin of any bosonic spin and charge excitation by using the Kac-Moody commutation relations. The charge bosons commute with the total spin operator S^2. Spin excitations are created by products of spin creation operators $b^\dagger_{m,s}$ acting on $|\omega_0\rangle$. The corresponding normalized states can be labelled by the set of which bosons were created $\{m_1, m_2, m_3, ...\}\rangle$, e.g. $|\{3,1,1\}\rangle = \frac{1}{\sqrt{2}} b^\dagger_{3,s} (b^\dagger_{1,s})^2 |\omega_0\rangle$. Therefore, the matrix elements of $\langle\{m_1, m_2, m_3, ...\}|S^2|\{m'_1, m'_2, m'_3, ...\}\rangle$ between any two such excitations can be evaluated uniquely by the Kac Moody algebra (A.8). The J^z_0 operators commute with all excitations and the ground state is characterized by $J^z_0|\omega_0\rangle = S^z|\omega_0\rangle = \frac{1}{2}|\omega_0\rangle$ in our case. For the $J^\pm$ operators we use the Kac-Moody relation in Eq. (A.8) with the help of computer algebra in order to successively commute them to the right until the action on the ground state is known. This results in a non-diagonal matrix for S^2 for each spin mode separately, which can be brought into diagonal form. The resulting eigenstates and eigenvalues are as follows:

$\mathbf{S = 1/2}$	$\lvert\omega_0\rangle$
$S = 1/2$	$\lvert\{1\}\rangle$
$S = 1/2$	$\sqrt{\frac{2}{3}}\lvert\{2\}\rangle + \sqrt{\frac{1}{3}}\lvert\{1,1\}\rangle$
$S = 3/2$	$-\sqrt{\frac{1}{3}}\lvert\{2\}\rangle + \sqrt{\frac{2}{3}}\lvert\{1,1\}\rangle$
$S = 1/2$	$\sqrt{\frac{1}{3}}\lvert\{3\}\rangle + \sqrt{\frac{2}{3}}\lvert\{1,1,1\}\rangle$
$S = 1/2$	$\sqrt{\frac{2}{9}}\lvert\{3\}\rangle + \sqrt{\frac{6}{9}}\lvert\{2,1\}\rangle - \sqrt{\frac{1}{9}}\lvert\{1,1,1\}\rangle$
$S = 3/2$	$-\sqrt{\frac{4}{9}}\lvert\{3\}\rangle + \sqrt{\frac{3}{9}}\lvert\{2,1\}\rangle + \sqrt{\frac{2}{9}}\lvert\{1,1,1\}\rangle$
$S = 1/2$	$-\sqrt{\frac{1}{3}}\lvert\{3,1\}\rangle + \sqrt{\frac{2}{3}}\lvert\{1,1,1,1\}\rangle$
$S = 1/2$	$\sqrt{\frac{12}{27}}\lvert\{4\}\rangle + \sqrt{\frac{2}{27}}\lvert\{3,1\}\rangle + \sqrt{\frac{12}{27}}\lvert\{2,1,1\}\rangle + \sqrt{\frac{1}{27}}\lvert\{1,1,1,1\}\rangle$
$S = 1/2$	$\sqrt{\frac{3}{54}}\lvert\{4\}\rangle + \sqrt{\frac{8}{54}}\lvert\{3,1\}\rangle + \sqrt{\frac{27}{54}}\lvert\{2,2\}\rangle - \sqrt{\frac{12}{54}}\lvert\{2,1,1\}\rangle + \sqrt{\frac{4}{54}}\lvert\{1,1,1,1\}\rangle$
$S = 3/2$	$-\sqrt{\frac{1}{3}}\lvert\{4\}\rangle + \sqrt{\frac{1}{3}}\lvert\{2,2\}\rangle + \sqrt{\frac{1}{3}}\lvert\{2,1,1\}\rangle$
$S = 3/2$	$-\sqrt{\frac{1}{6}}\lvert\{4\}\rangle + \sqrt{\frac{4}{9}}\lvert\{3,1\}\rangle - \sqrt{\frac{1}{6}}\lvert\{2,2\}\rangle + \sqrt{\frac{2}{9}}\lvert\{1,1,1,1\}\rangle$

for the case that the state $|\omega_0\rangle$ has total spin of $S = 1/2$.

It is also possible to consider a $|\omega_0\rangle$ state with $S = 0$. In that case the eigenstates are given by:

$\mathbf{S = 0}$	$\lvert\omega_0\rangle$
$S = 1$	$\lvert\{1\}\rangle$
$S = 0$	$\lvert\{1,1\}\rangle$
$S = 1$	$\lvert\{2\}\rangle$
$S = 0$	$\lvert\{2,1\}\rangle$
$S = 1$	$\lvert\{3\}\rangle$
$S = 1$	$\lvert\{1,1,1\}\rangle$
$S = 0$	$\sqrt{\frac{2}{3}}\lvert\{3,1\}\rangle + \sqrt{\frac{1}{3}}\lvert\{1,1,1,1\}\rangle$
$S = 0$	$\sqrt{\frac{1}{9}}\lvert\{3,1\}\rangle + \sqrt{\frac{2}{3}}\lvert\{2,2\}\rangle - \sqrt{\frac{2}{9}}\lvert\{1,1,1,1\}\rangle$
$S = 1$	$\lvert\{4\}\rangle$
$S = 1$	$\lvert\{2,1,1\}\rangle$
$S = 2$	$-\sqrt{\frac{2}{9}}\lvert\{3,1\}\rangle + \sqrt{\frac{1}{3}}\lvert\{2,2\}\rangle + \sqrt{\frac{4}{9}}\lvert\{1,1,1,1\}\rangle$
$S = 0$	$\sqrt{\frac{4}{7}}\lvert\{4,1\}\rangle + \sqrt{\frac{3}{7}}\lvert\{2,1,1,1\}\rangle$
$S = 0$	$\sqrt{\frac{6}{63}}\lvert\{4,1\}\rangle + \sqrt{\frac{49}{63}}\lvert\{3,2\}\rangle - \sqrt{\frac{8}{63}}\lvert\{2,1,1,1\}\rangle$
$S = 1$	$\lvert\{5\}\rangle$
$S = 1$	$\lvert\{3,1,1\}\rangle$
$S = 1$	$\lvert\{2,2,1\}\rangle$
$S = 1$	$\lvert\{1,1,1,1,1\}\rangle$
$S = 2$	$-\sqrt{\frac{1}{3}}\lvert\{4,1\}\rangle + \sqrt{\frac{2}{9}}\lvert\{3,2\}\rangle + \sqrt{\frac{4}{9}}\lvert\{2,1,1,1\}\rangle$